Spatial–Temporal Change of a Dam Lake Using Remote Sensing and Meteorological Drought Indices

Emre Özelkan

1 Introduction

Drought, defined as lack of water in a certain period, is a natural disaster of meteorological origin that affects our lives dramatically in ecological, sociological, economic and many other areas (Özelkan 2016; Özelkan 2019a). Drought progresses slowly, its beginning and end are very difficult to predict, and its effects continue for a long time (Wilhite 2020). Drought first affects natural resources such as water, agricultural area and forest. An increasing population, the increased need for natural resources and excessive consumption have made combating drought more important than ever, especially in arid and semi-arid climatic regions (Genc et al. 2011; Çamoğlu et al. 2018; Çakaroz et al. 2020).

Drought is a four-stage process that begins with a lack of precipitation, and its first stage is called meteorological drought (Mishra et al. 2010; Özelkan 2019a). The second stage is hydrological drought, expressed as a shortage of water resources (Mishra et al. 2010; Kapluhan 2013; Özelkan 2019a). The third stage is agricultural drought, which refers to the adverse conditions in agricultural production such as loss of product and yield (Mishra et al. 2010; Kapluhan 2013; Özelkan 2019a). The last stage of drought is the impact of meteorological, hydrological and agricultural drought on social and economic life (unemployment, migration, economic depression, unrest, poverty, etc.) and this is referred to as socio-economic drought (Mishra et al. 2010; Kapluhan 2013; Özelkan 2019a). Considering the destructive effects, every stage of drought should be carefully examined, modeled and necessary precautions should be taken. In this context, the present research examined the effect of meteorological drought on water resources.

E. Özelkan (✉)
Faculty of Architecture and Design, Department of Urban and Regional Planning, School of Graduate Studies, Risk Management of Natural Disasters Program, Çanakkale Onsekiz Mart University, 17020 Çanakkale, Turkey
e-mail: emreozelkan@comu.edu.tr

A. Shaban (ed.), *Satellite Monitoring of Water Resources in the Middle East*,
Springer Water, https://doi.org/10.1007/978-3-031-15549-9_9

The most common methods used to determine meteorological drought are meteorological drought indices, which are calculated according to equations that include meteorological parameters such as temperature, precipitation and humidity (Mohammed and Scholz 2017). Some of the major meteorological drought indices can be listed as Standard Precipitation Index (SPI) (McKee et al. 1993), Standard Precipitation Evapotranspiration Index (SPEI) (Vicente-Serrano et al. 2010), Percent of Normal Index (PNI) (Willeke 1994), Reconnaissance Drought Index (RDI) (Tsakiris 2005) and Palmer Drought Severity Index (Palmer 1965). The cumulative deviation curve is a frequently preferred method to determine the change and behavior of drought from past to present and to make predictions for the future (Liu et al. 2019; Özelkan 2019a, b). In addition to meteorological drought, excessive evapotranspiration and human activities (daily consumption, irrigation, energy production, etc.) that occur in water resources such as lakes and streams may also cause hydrological drought (Li et al. 2017; Veijalainen et al. 2019). Losses that occur in water resources can be determined by many methods such as water level measurements (Yıldız and Deniz 2005), hydrometeorological calculations (Penman–Monteith, Thornthwaite, etc.) (Lang et al. 2017), empirical open water surface evaporation calculations (Dalton, Meyer, etc.) (Gorjizade et al. 2014), water balance and budget calculations (Yaykiran et al. 2019), heat and mass transport (Zannouni et al. 2017), and energy balance (Duan and Bastiaanssen 2017).

In the monitoring and management of water resources, satellite remote sensing is frequently and successfully used (McFeeters 1996; Xu 2006; Özelkan 2019b; Karaman 2021). Satellite remote sensing, which can view wide areas at once and conveniently provide the rapid and detailed examination of large water bodies (Karaman et al. 2015; Kale and Acarlı 2019a, b; Karaman 2022). Therefore, remote sensing has become a very useful tool in determining and modeling hydrological drought (Özelkan and Karaman 2018a; Schultz and Engman 2019). Water indices produced from spectral bands of remote sensing data, with their simple algorithms, have become one of the most preferred methods for determining water bodies (Ji et al. 2015; Özelkan 2020). The normalized difference water index (NDWI), created by considering the difference between the high reflectance of water in the green region and the low reflection in the near infrared (NIR) region, is one of the most frequently used water body detection and analysis indices for satellite remote sensing (McFeeters 1996; Karaman and Özelkan 2022). Following these, many different water indices have been presented to determine water bodies, such as the modified NDWI (MNDWI) generated using the short-wave infrared (SWIR) instead of the NIR in the NDWI (Xu 2006), and the automated water extraction index (AWEI) that additionally considers reflection in the blue region (Feyisa et al. 2014). However, correlation and verification of the remote sensing findings with meteorological and hydrological drought indicators calculated by in-situ measurement values make remote sensing studies more meaningful (Özelkan and Karaman 2018a).

In this study, the spatial–temporal change of a dam lake area was monitored by satellite remote sensing and the influence of meteorological drought on this areal change was examined. The Atikhisar Dam Lake, which is near the city of Çanakkale and the only water source that feeds the region, was preferred as the study area. The

areal change of the dam lake was determined by using NDWI derived from multi-spectral Landsat satellite images. The temporal change of the drought is presented by the cumulative deviation curve. To determine meteorological drought, SPI and SPEI drought indices were utilised comparatively. The study covers the period between 1984 and 2020 and all calculations were made according to the 12-month water year calendar, which begins on the first day of October and ends at the end of September. In conclusion, this study reveals how successfully the areal change of a dam lake influenced also by anthropogenic effects such as daily consumption, irrigation and energy production, can be modeled by considering only the meteorological drought.

2 Materials and Methods

This section explains the general characteristics of the study area, meteorological and remote sensing data used, processing of these data, meteorological and remote sensing indices produced and how the analysis was carried out.

2.1 Study Area

Atikhisar Dam Lake is located between 26°31′2.22"–26°33′10.30"E eastern meridians and 40°3′49.67"–40°7′36.31" northern parallels and within Çanakkale province in the west of Turkey (Fig. 1). Atikhisar Dam Lake is the only water source of Çanakkale city and used for several purposes such as for drinking water, irrigation and flood protection (Akbulak et al., 2008; Koca, 2005). The dam was built between 1971 and 1975 as a body of earth fill on Sarıçay Creek, which is within the boundaries of the Sarıçay Basin (Akbulut et al. 2009). Saricay Basin covers an area of approximately 473 km^2 with a maximum height of 908 m and a slope of 45.7°. Saricay Creek is the longest stream in the basin and is approximately 43 km long and 8.5 km of it within the dam's limits. Saricay Creek then passes through the middle of the city and flows into the Çanakkale Strait (Dardanelles) (Özelkan 2020). Atikhisar Dam Lake is situated 11 km from Çanakkale city center, 60 m above sea level, has an area of more than 3 km^2 at normal water elevation, and an average volume of 40 hm^3 (Koca 2005). It has been recorded that the water availability in the dam lake has decreased to 10% of its normal level due to severe droughts experienced in the past (Koca 2005).

The study area is under the influence of the subtropical Mediterranean climate zone (Altan and Türkeş 2015). More particularly, the regional mild Marmara climate, a transition zone from the Black Sea to the Mediterranean, is experienced in the invetigated region (Şensoy et al. 2018). According to the long-term data of the Turkish State Meteorological Service, the most rainy month is December with an average monthly total of 106.8 mm, and the driest period is August with 6.4 mm. July is the hottest month with an average of 25 °C and the coldest month is January with 6.1 °C.

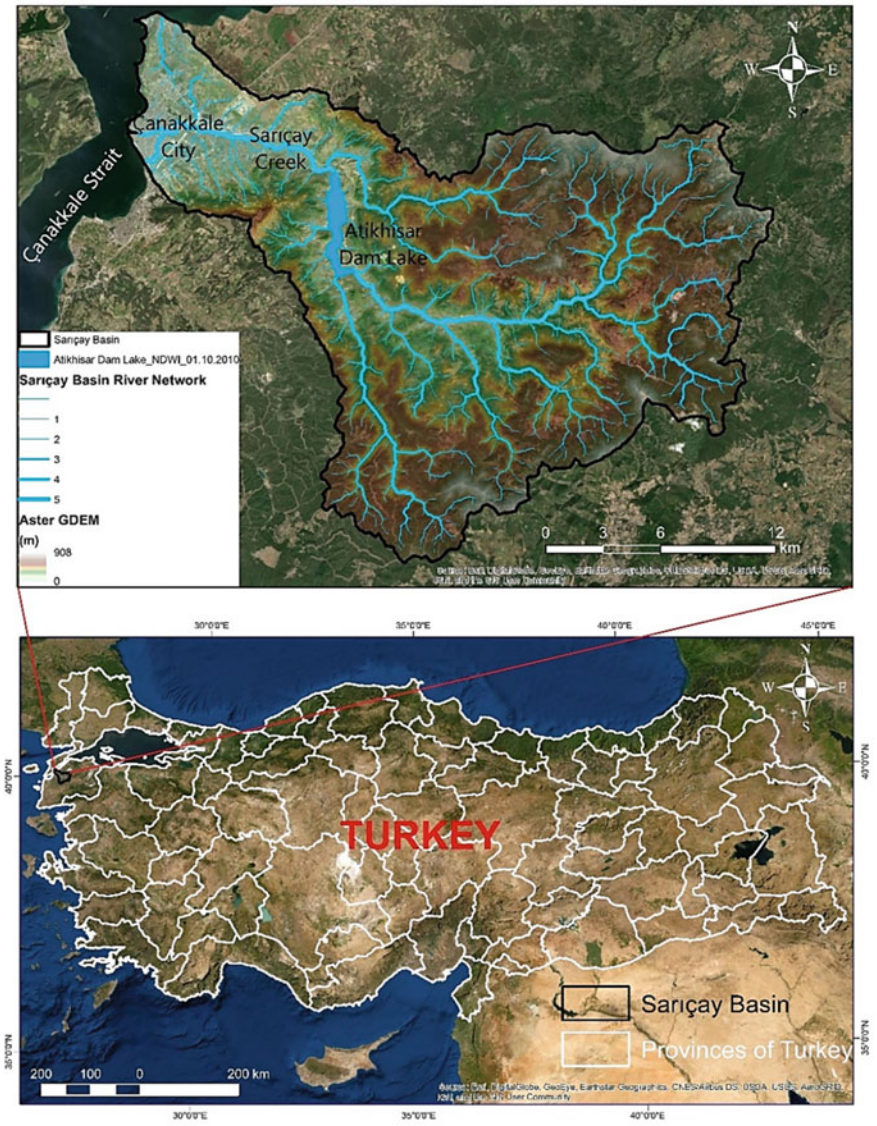

Fig. 1 Location of study area

Winds from the north cause low temperatures in winter while winds from the south bring precipitation to the region (Ilgar 2010). Around the dam lake vicinity are found the flora olea oleaster, laurus nobilis, guercus coccifera, rhus coriaria, pinus brutia and pinus nigra growing, which are maquis elements belonging to Mediterranean vegetation. In the northern slopes of the dam lake are the species guercus, fagus

orientalis and castanea sativaunder which thrive under the influence of humid mild forests (Koca 2005).

2.2 Meteorological Data and Pre-processing

The precipitation and temperature data measured between 1984 and 2020 at the meteorological station of the Turkish State Meteorological Service located in the center of Çanakkale city were used to determine the drought in the study area. All investigations were performed according to the 12-month water year calendar, starting at the beginning of October (i.e., beginning of rainy season) and ending at the end of September (i.e., end of dry season). For example, the 12-month period between October 1983 and September 1984 was included in the 1984 water year data.

The temporal change (length, frequency, trend, etc.) of the drought experienced in the region was firstly examined using the cumulative deviation curve. The cumulative deviation is calculated as the sum of deviations of the total precipitation for each period (water year in this study) from the long-term average of the investigated time interval (1984–2020 in this study) and reveals the dry and rainy periods in the time interval investigated (Sener et al. 2010; Özelkan and Karaman 2018b; Özelkan 2019a). The cumulative deviations are calculated using the Eq. 1 and graphically drawn as a function of t, with t = 1, 2, …, n (Karabulut 2015).

$$S_t = \sum_1^t (X_i - X_m) \tag{1}$$

where S_t is the sum of deviations, X_i is the total precipitation of each period, and X_m is the long-term average of the investigated time interval. The lower and upper safety limits of the precipitation and coefficient of variation (Cv), in which small values indicate regions with regular and enough precipitation, are used in the interpretation of the cumulative deviation, and are calculated by using X_m and standard deviation (σ) of the long-term data, as follows (Türkeş 2010; Yetmen 2013; Yolcubal 2019).

$$\text{Lower safety limit} = X_m - \sigma \tag{2}$$

$$\text{Upper safety limit} = X_m + \sigma \tag{3}$$

$$Cv = \sigma / X_m \tag{4}$$

The meteorological drought was determined by using the Standard Precipitation Index (SPI) and Standard Precipitation Evapotranspiration Index (SPEI). SPI

is computed by dividing the difference of the corresponding period's (water year in this study) (X_i) precipitation total from the long-term average (X_m) of totals by the standard deviation value (σ) calculated from the long-term data (McKee et al. 1993; Dhakar et al. 2013; Özelkan et al. 2016).

$$SPI = (X_i - X_m)/\sigma \tag{5}$$

SPEI takes into account both precipitation and temperature variability to predict drought conditions (Vicente-Serrano et al. 2010). The first step in calculating the SPEI proposed by Vicente-Serrano is to estimate the monthly potential evapotranspiration (PET) using the simple and useful Thornthwaite method (Vicente-Serrano et al. 2010; Danandeh and Vaheddoost 2020). Afterwards, the water surplus or deficit (D_i) of the corresponding month (i) is computed using the water balance equation that calculates the difference between precipitation (P_i) and PET_i (Vicente-Serrano et al. 2010; Danandeh and Vaheddoost 2020).

$$D_i = P_i - PET_i \tag{6}$$

Then, the evolved water deficit values (D_i) are standardized, and finally fitted to a log-logistic distribution (Vicente-Serrano et al. 2010; Danandeh and Vaheddoost 2020). The SPEI value of the corresponding month (i) is the standardized value of the exceeding probability (p) of a given D_i (Danandeh and Vaheddoost 2020).

$$SPEI = W_i - \frac{2.515517 + 0.802853W_i + 0.010328{W_i}^2}{1 + 1.432788W_i + 0.189269{W_i}^2 + 0.001308{W_i}^3} \tag{7}$$

If $p \leq 0.5$, $W_i = \sqrt{-2\ln(p)}$, and if $p > 0.5$, $W_i = \sqrt{-2\ln(1-p)}$, the sign of the resultant SPEI is reversed where p is the probability of exceeding a designated D value, and $p = 1 - F(x)$. SPI and SPEI can be used to study meteorological drought for 1, 3, 6, 9, 12 and 24-month periods (McKee 1993; Vicente-Serrano et al. 2010; Arslan et al. 2016; Osuch et al. 2016). In this study, 12-month SPI and SPEI values covering the water year were calculated. The positive values of the SPI and SPEI represent the rainy periods without drought, while the negative values represent the drought periods with less precipitation. The drought classes (i.e., climatic moisture categories) and values are shown in Table 1.

2.3 Remote Sensing Data and Pre-processing

A total of 33 multispectral Landsat satellite images (path/row: 173/34) with 16 bit radiometric and 30 m spatial resolution were obtained between 1984 and 2018 over the study area from the United States Geological Survey (USGS) data portal (Table 2). Note that all images are provided at the end of the water year to be consistent with

Table 1 Meteorological drought classes and values of SPI and SPEI (Liu et al. 2021)

Drought class	Drought values
Extremely wet	≥ 2
Severely wet	$1.5 \leq \text{SPI} \leq 1.99$
Moderately wet	$1.0 \leq \text{SPI} \leq 1.49$
Normal	$-0.99 \leq \text{SPI} \leq 0.99$
Moderate drought	$-1.49 \leq \text{SPI} \leq -1.00$
Severe drought	$-1.99 \leq \text{SPI} \leq -1.5$
Extreme drought	≤ -2.00

Table 2 List of Landsat satellite images used in study

No	Acquisition date	Satellite	Path/Row
1	07.09.1984	Landsat 5 TM	181/032
2	26.09.1985	Landsat 5 TM	181/032
3	13.09.1986	Landsat 5 TM	181/032
4	23.09.1987	Landsat 5 TM	182/032
5	25.09.1988	Landsat 5 TM	182/032
6	07.10.1989	Landsat 5 TM	181/032
7	01.10.1990	Landsat 5 TM	182/032
8	27.09.1991	Landsat 5 TM	181/032
9	29.09.1992	Landsat 5 TM	181/032
10	23.09.1993	Landsat 5 TM	182/032
11	19.09.1994	Landsat 5 TM	181/032
12	24.09.1996	Landsat 5 TM	181/032
13	04.10.1997	Landsat 5 TM	182/032
14	30.09.1998	Landsat 5 TM	181/032
15	17.09.1999	Landsat 5 TM	181/032
16	19.09.2000	Landsat 5 TM	181/032
17	30.09.2001	Landsat 7 ETM +	181/032
18	24.09.2002	Landsat 7 ETM +	182/032
19	05.10.2003	Landsat 5 TM	182/032
20	30.09.2004	Landsat 5 TM	181/032
21	03.10.2005	Landsat 5 TM	181/032
22	04.09.2006	Landsat 5 TM	181/032
23	30.09.2007	Landsat 5 TM	182/032
24	05.10.2009	Landsat 5 TM	182/032
25	01.10.2010	Landsat 5 TM	181/032
26	04.10.2011	Landsat 5 TM	181/032
27	30.09.2013	Landsat 8 OLI	182/032

(continued)

Table 2 (continued)

No	Acquisition date	Satellite	Path/Row
28	19.10.2014	Landsat 8 OLI	182/032
29	20.09.2015	Landsat 8 OLI	182/032
30	01.10.2016	Landsat 8 OLI	181/032
31	18.09.2017	Landsat 8 OLI	181/032
32	01.10.2019	Landsat 8 OLI	182/032
33	03.10.2020	Landsat 8 OLI	182/032

the drought index results. In 1995, 2008, 2012 and 2018, cloudless images could not be obtained at the end of the water year. However, 33 images were obtained consisting of 24 Landsat-5 Thematic Mapper (TM), 2 Landsat-7 Enhanced Thematic Mapper (ETM +) and 7 Landsat-8 Operational Land Imager (OLI) images. Furthermore, atmospheric and geometric corrections of all images representing surface reflectance were made by the vendor.

The NDWI of McFeeters (1996), which takes into account the high reflectance in the visible region and low reflectance in the infrared of the water, was preferred to determine the lake area, since NDWI gives better results in natural areas (i.e., water, vegetation, mud and soil) compared to MNDWI indices that work with SWIR (Özelkan 2020). NDWI ranges from −1 to 1 and values above 0 indicate water (McFeeters 1996). The NDWI index was first proposed for Landsat 5 TM (McFeeters 1996), then numerous water body determination studies were performed using Landsat 7 ETM + (Zhou et al. 2017; Özelkan 2019a) and Landsat 8 OLI (Özelkan 2019b; Yang et al. 2015). NDWI images are generated by replacing the second and fourth bands of Landsat 5 TM and Landsat 7 ETM + and the third and fifth bands of Landsat 8 OLI satellite images in Eq. 8, in which R means reflectance. The NDWI index is expressed in Eqs. 9, 10 and 11 with the center wavelengths in micrometers of green and NIR bands for each satellite as follows:

$$NDWI = \frac{(R_{Green} - R_{NIR})}{(R_{Green} + R_{NIR})} \tag{8}$$

$$NDWI_{Landsat5TM} = \frac{(R_{0.5690} - R_{0.8400})}{(R_{0.5690} + R_{0.8400})} \tag{9}$$

$$NDWI_{Landsat7ETM+} = \frac{(R_{0.5600} - R_{0.8350})}{(R_{0.5600} + R_{0.8350})} \tag{10}$$

$$NDWI_{Landsat8OLI} = \frac{(R_{0.5613} - R_{0.8646})}{(R_{0.5613} + R_{0.8646})} \tag{11}$$

2.4 Data Analysis

Between 1984 and 2018, at the end of the water year (i.e., at the end of the dry period), 33 lake area values extracted from NDWI created from Landsat satellite images were associated with 33 SPI and SPEI meteorological drought indices values respectively for the same period by correlation-regression analysis. In this context, Pearson's correlation coefficient (r) and significance probability (p) values of ANOVA (Analysis of Variance) (i.e., significance F (SF)) were calculated among the data sets. Additionally, root mean square error (RMSE) was used to determine the accuracy of the water body areas derived from NDWI compared to areas measured by the Turkish State Hydraulic Works.

3 Results and Discussion

In this section, the spatial–temporal change of meteorological drought and dam lake area will be examined, and the findings will be discussed by considering the field data and previous studies.

3.1 Meteorological Drought Analysis

The trend and frequency of the meteorological drought in the study area is presented by the cumulative deviation curve analysis (Fig. 2). The average precipitation in the study area, which is under the influence of the subtropical Mediterranean climate zone, is 581 mm and its standard deviation is 136 mm. The lower and upper safety limits of the precipitation are 718 mm and 445 mm, respectively. The 1985, 1990, 1992, 2007, 2008 and 2020 values are under the lower safety limit, and the minimum precipitation was experienced in 2008 with 333 mm. The precipitations of 1995, 1998, 2002, 2013 and 2018 were over the upper safety limits, and the maximum was experienced in 2013 with 844 mm. Between 1984 and 2020, 70.27% of the precipitation of 37 water years was found to be within the safety limits. The coefficient of variation (Cv) was found as 0.23, indicating that the region receives regular and sufficient precipitation. On the other hand, in the last two decades it has been observed that the difference between minimum and maximum precipitation has increased (i.e., the σ tends to grow) and the precipitation regime has begun to deteriorate, although there is a small increase in the average annual precipitation totals covering the long term. Change in precipitation patterns is an obvious indicator of climate change (Dore 2005; Kale and Acarlı 2019b). Moreover, small Cv value 0.23 indicates that changes in groundwater levels are also more regular in water wells located in such regions (Yolcubal 2019).

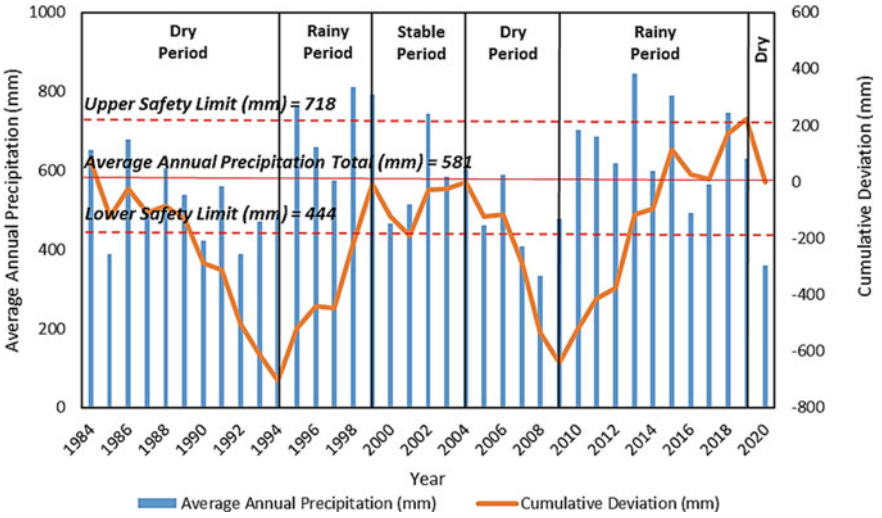

Fig. 2 Cumulative deviation curve from water year precipitation data between 1984 and 2020

According to the cumulative deviation curve graph created from the total water year precipitation data between 1984 and 2020 (Fig. 2), a long dry period occurred between 1984 and 1994, followed by a rainy period until 1999, then a partially stable period until 2004, a dry period between 2004 and 2010, then a long rainy period between 2010 and 2019 were experienced in the study area. It should be noted that the dry period until 1994 begins in 1982. Since before 1984 was not included in the period investigated, it has been excluded from the analysis. Finally, the past (1984–2019) behavior and current trend of the curve indicate that a dry period was entered as of 2019. In the analyzed period, the least precipitation after 2008 was 360 mm in 2020, just after 2019 with 630 mm. This sharp decrease in precipitation from 2019 to 2020 may indicate that the dry period we are in currently may be extremely severe in the coming years.

The temporal variation of drought was examined according to the 12-months SPI (SPI-12) and SPEI (SPEI-12) drought values calculated from the total precipitation of the water year and shown together with the dry and rainy periods according to the cumulative deviation curve (Fig. 3). SPI and SPEI values generally exhibit similar behavior as the cumulative deviation curve in the long term and are naturally more correlated with the precipitation. The average of differences between SPI and SPEI values is 0.18 and the biggest difference is 0.51. Pearson's correlation coefficient (r) between SPI and SPEI is 0.97. It was observed that SPI and SPEI values differ more in arid conditions below zero, while this difference is less in rainy periods, which are expressed with values above zero. Compared to SPEI, SPI generally gives more extreme values due to lack of precipitation in arid conditions. According to SPI and SPEI, the most severe drought years were determined as 2008 and 2020, respectively. As mentioned, a dry period was entered after 2019 and the severe drought in 2020

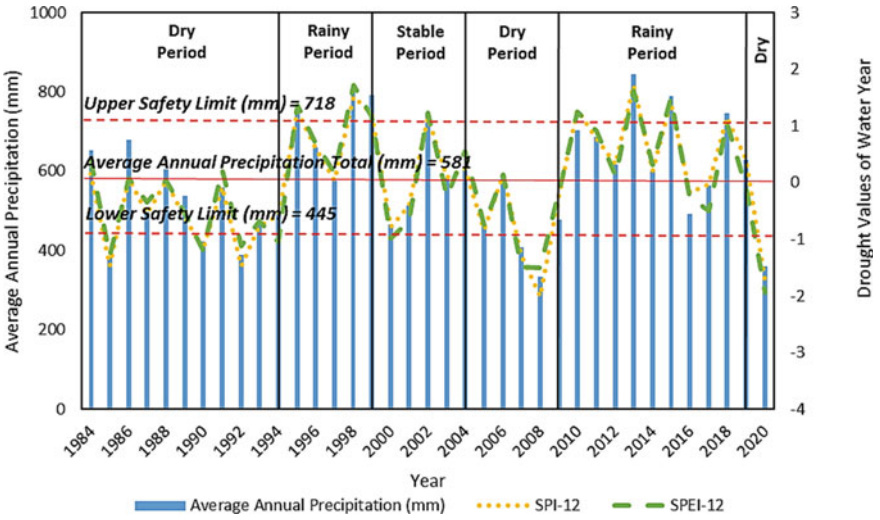

Fig. 3 SPI and SPEI drought values from water year precipitation data between 1984 and 2020

(SPI $= -1.74$ and SPEI $= -1.94$) at the beginning of the dry period is a worrying precursor for coming years.

3.2 Determination of Lake Area Using Remote Sensing and Its Correlation with Drought

The spatial–temporal changes of the water body area in the dam lake were examined with NDWI generated from the Landsat satellite images obtained at the end of the water years between 1984 and 2020 (Fig. 4). Since cloudless images are not available for 1995, 2008, 2012 and 2018, these four years were excluded from the analysis in determining the correlation of the lake area with drought. Within the analyzed NDWI data set, the average of the lake water area is 2.02 km^2 and the standard deviation is 0.61 km^2. The lake area reached its widest limits in 2010 with 2.98 km^2. According to the water body area values determined from local measurements by the Turkish State Hydraulic Works, the lake area was determined by NDWI to have an average of 5.78 km^2 RMSE, with 82.68% accuracy. The driest year hydrologically (i.e., the year with the smallest lake area) was determined as 1990 with a lake water area of 1.09 km^2, even though the driest years meteorologically were 2008 (not included in analysis) and 2020 (Fig. 5). Despite the severe meteorological drought in 2020, the reason why the water area is larger than in 1990 is the improvement and modernization of agricultural irrigation systems (i.e., preferring drip and sprinkler irrigation instead of wild flooding systems) over the years and the decrease in water consumption.

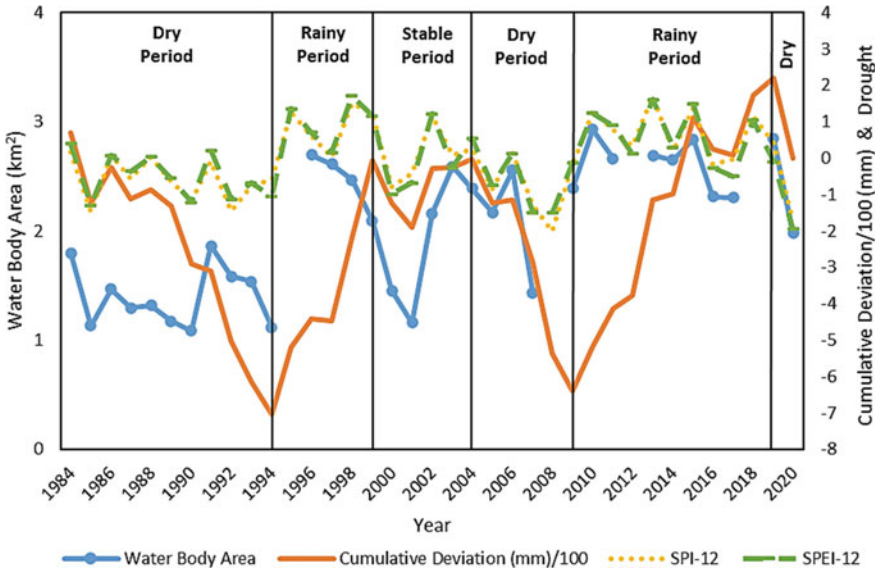

Fig. 4 The spatial–temporal change of water body area of Atikhisar Dam Lake, cumulative deviation, SPI and SPEI values. (Note: Cumulative deviation values were divided by 100 to display together with water body area, SPI and SPEI values.)

Similar to meteorological drought, hydrologically, the driest period was between 1984 and 1994 with an average of 1.4 km^2, and the rainy period was between 2010 and 2019 with an average of 2.62 km^2. Especially at the end of the water year, there was a 26% increase in the average precipitation in September between 2010 and 2019 compared to the 1980s, and this precipitation increase is a major factor in the increase of the lake area (Fig. 5). At the end of the water years since 2009, the lake area decreased below 2 km^2 for the first time in 2020. The 30.5% decrease from 2.85 km^2 in 2019 to 1.98 km^2 in 2020 at the beginning of the dry period creates concern regarding the coming years (Fig. 5). The lake area determined by NDWI at the transition dates to rainy or dry periods according to the cumulative deviation curve, and the minimum and maximum water body area of the lake within the data set for the examined dates, are shown in Fig. 5.

When the temporal variation of the data was examined, it was seen that the change in the lake area is related to meteorological drought (Fig. 4). However, since the cumulative deviations are computed as the sum of the differences of precipitation from the mean and are not suitable for short-term interpretation (annually, in this study), they were found to be uncorrelated with the lake areas determined by remote sensing (Fig. 6a). However, in the long-term analysis, there is a significant relationship in the trend between cumulative deviation and the area values (Fig. 4). Compared to cumulative deviation values, the change in the SPI and SPEI drought values were found to be significantly more correlated with the change in the water body area (Fig. 6b, c). According to ANOVA, the SF values between the water body area and drought

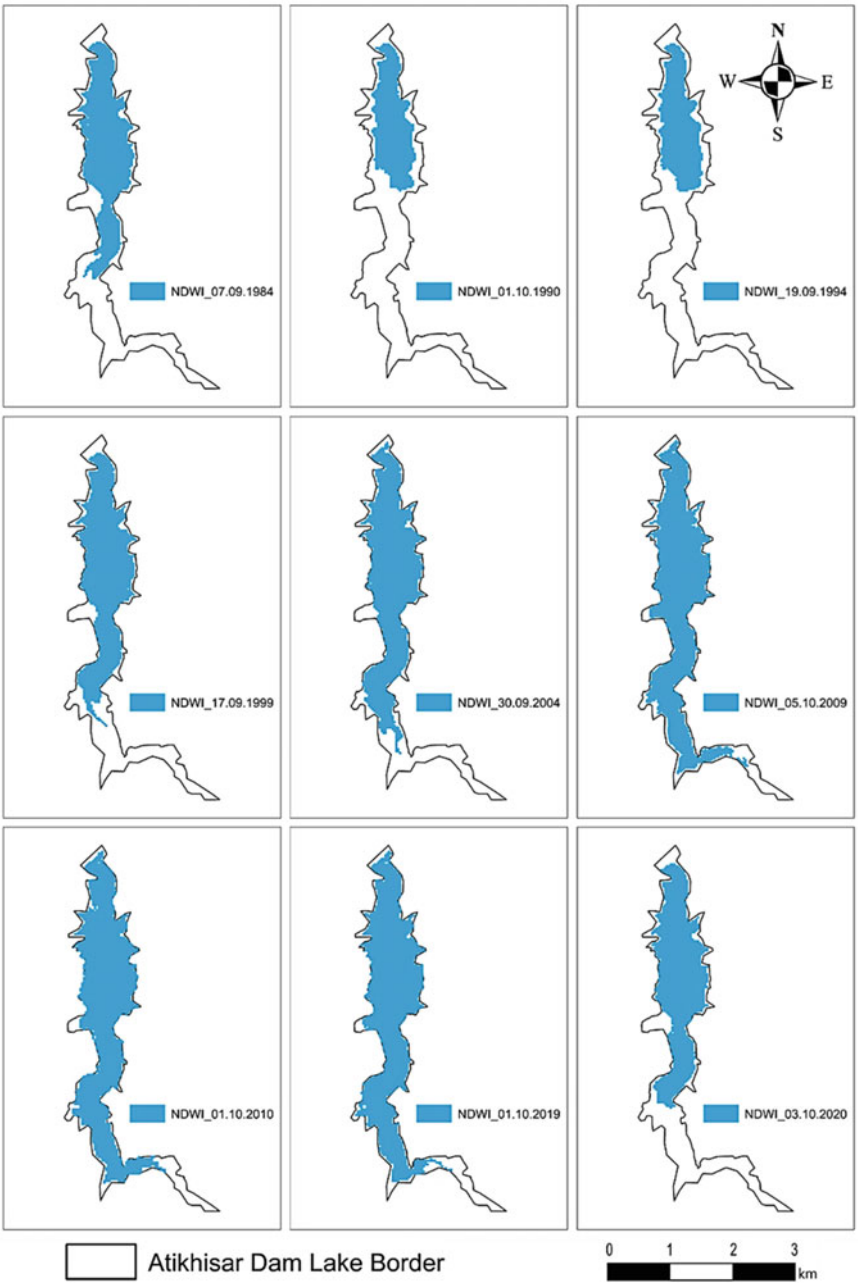

Fig. 5 Areas of lake determined by NDWI on transition date to a rainy or dry period, according to cumulative deviation curve. (Note: 1990 and 2010 represent minimum and maximum areas of lake, respectively, within data set examined.)

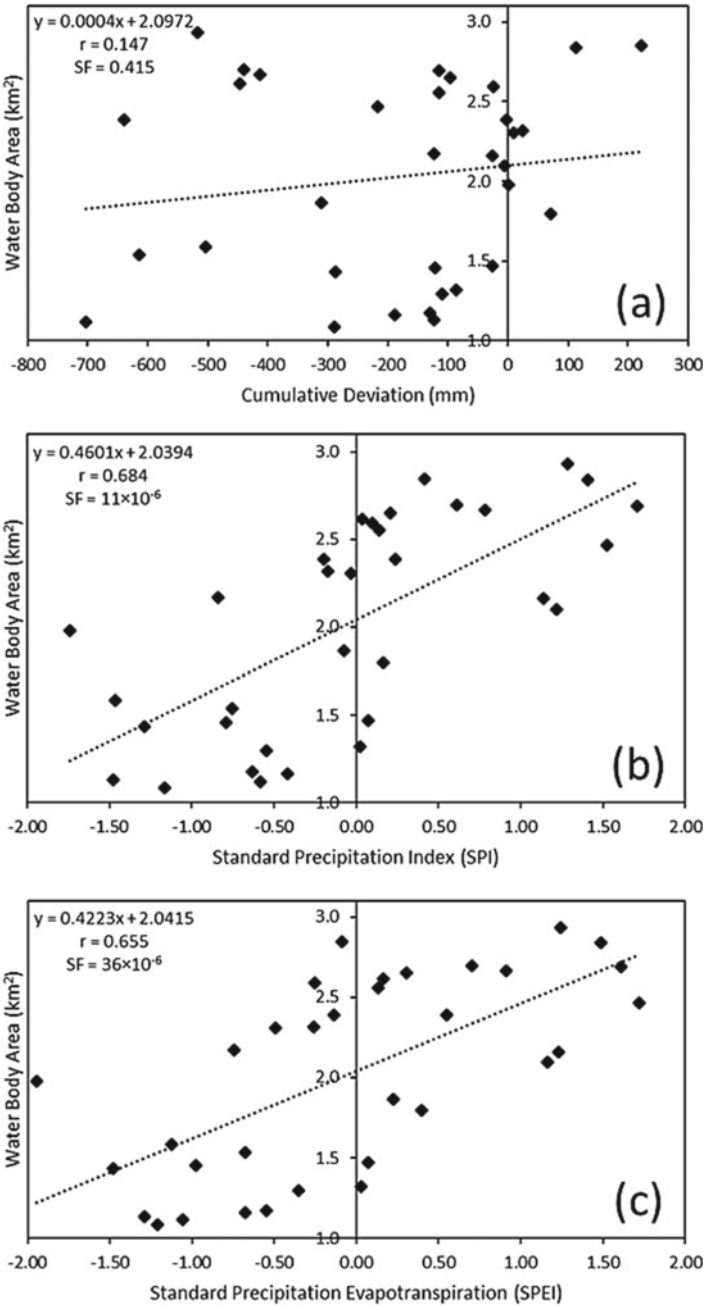

Fig. 6 Correlation between water body area from NDWI and **a** cumulative deviation, **b** SPI, and **c** SPEI values

indices (i.e., SPI and SPEI) were found to be almost 0, and all correlations shown in Fig. 6b, c have almost 100% confidence level. SPI values with 0.68 correlation were found to be slightly more correlated with the water body area values from NDWI than SPEI with 0.65. SPI may have generated better results because the valley where the dam is located is narrow, far from the sea, and richly forested in vegetation. Therefore, the wind triggering evapotranspiration is not high in the region and as a result rainfall is more dominant in the water budget.

The imperfect correlations show that the dam lake area not only changes due to meteorological drought. Atikhisar Dam Lake is multi-purpose and was built to provide drinking water, agricultural irrigation and flood protection (Koca 2005; Akbulak et al. 2008; Kale and Acarlı 2019b). On the other hand, the population of Çanakkale city has increased approximately 120 times since the initial construction of the dam and more than 30% in just the last 10 years (TÜİK 2020; Özelkan et al. 2018). While this population growth has caused an increase in anthropogenic demand (i.e., water consumption) from the dam lake, it may result in a decrease in the correlation between the water body area of the lake and meteorological drought. Preventing floods that may threaten the city of Çanakkale and agricultural areas, and leaving excess water accumulated in the lake due to precipitation, are other important tasks of the Atikhisar Dam (Koca 2005; Kale and Acarlı 2019b) that may also cause a decrease in the correlations. In addition, when examined in terms of flora, the vegetation density around the dam prevents erosion and prolongs the life of the dam. Conversely, dense vegetation slows down surface flow in the Sarıçay Basin, where the dam is located, and increases the groundwater level, which causes a decrease in the water reaching the dam lake (Koca 2005). The findings listed so far strongly suggest that the presence of water in the lake area may not be solely due to meteorological drought.

Finally, since the change of drought over the long term was examined in this study, 30 m was preferred as the common spatial resolution used in NDWI data produced from different Landsat satellites. However, with 15 m resolution the lake area can be determined more successfully (Özelkan, 2020), and this may increase the correlation between the lake area and drought in this study. Additionally, since the water area values created from the NDWI images are associated with SPI and SPEI calculated based on water year meteorological data, the time difference between the image acquisition dates and the end of the water year may affect the correlations.

4 Conclusions

The ever-increasing population worldwide together with severe drought puts tremendous pressure on water resources. Particularly in arid and semi-arid regions, the influence of drought on water resources should be carefully monitored and examined in all aspects. In other words, water resources management should be the most important issue in drought-prone regions; implementing urgent precautions such as education of the public on water management, a preference for technologies that consume less

water in our lives and industry, strict control of agricultural irrigation and usage of sensitive methods, and preference of agricultural plants that do not consume excessive water according to climatic characteristics. Otherwise, it is inevitable that we will experience a lack of drinking water and food. Misguided water management causes meteorological drought to evolve into hydrological, agricultural and eventually socio-economic drought. In this study, the correlation between spatial–temporal change in a dam lake and meteorological drought was investigated. While the cumulative deviation curve, SPI and SPEI were used to determine the meteorological drought, NDWI was used to determine the water change in the lake area. The main findings of this study are as follows.

- The cumulative deviation curve was very convenient in the interpretation of meteorological drought over a long period.
- SPI and SPEI gave precise results in the interpretation of meteorological drought in short periods.
- The drought values generated by SPI and SPEI were significantly correlated with the water area values of the lake determined by NDWI. Since the valley where the dam is located may have made evaporation slightly less important than precipitation, SPI gave a slightly better result than SPEI.
- Since the investigated reservoir is not a natural lake but a dam lake, meteorological drought cannot be said to be the only determinant factor in changes in the water body area.

This study shows that in order to create more successful models, the water budget of the dam lake (water consumption, irrigation, discharged water, etc.) as well as hydrogeological and environmental factors should be considered. The results of this study proved that the ability to ensure continuous monitoring, view large areas at once, and construct digital data easily associated with different sources of data make remote sensing a very successful tool to monitor and examine the impact of drought on water resources.

Acknowledgements The author would like to thank the USGS for the Landsat data, the Turkish State Hydraulic Works for the hydrological data, the Turkish State Meteorological Service for the meteorological data.

References

Akbulak C, Erginal A, Gönüz A, Öztürk B, Çavuş C (2008) Investigation of land use and coastline changes on the Kepez delta using remote sensing. J Black Sea/Mediterranean Environ 14(2):95–106

Akbulut M, Odabaşı DA, Kaya H, Çelik ES, Yıldırım MZ, Odabaşı S, Selvi K (2009) Changing of Mollusca fauna in comparison with water quality: Saricay Creek and Atikhisar reservoir models (Canakkale-Turkey). J Anim Vet Adv 8(12):2699–2707

Altan G, Türkeş M (2015) Hydroclimatologic characteristics of the forest fires occurred at the Çanakkale district and relationship with climate variations. Aegean Geograph J 20(2):1

Arslan O, Bilgil A, Veske O (2016) Meteorological drought analysis in Kizilirmak basin using standardized precipitation index method. Nigde Omer Halisdemir Univ J Eng Sci 5(2):188–194
Çakaroz D, Özelkan E, Karaman M (2020) Investigation of the effect of drought on temporal change in wetlands determined by remote sensing: the case study in Umurbey Delta (Çanakkale). Eur J Sci Technol 20:898–916. https://doi.org/10.31590/ejosat.799717
Çamoğlu G, Demirel K, Genc L (2018) Use of infrared thermography and hyperspectral data to detect effects of water stress on pepper. Quant InfraRed Thermograph J 15(1):81–94
Danandeh Mehr A, Vaheddoost B (2020) Identification of the trends associated with the SPI and SPEI indices across Ankara, Turkey. Theor Appl Climatol 139:1531–1542. https://doi.org/10.1007/s00704-019-03071-9
Dhakar R, Sehgal VK, Pradhan S (2013) Study on inter-seasonal and intra-seasonal relationships of meteorological and agricultural drought indices in the Rajasthan State of India. J Arid Environ 97:108–119
Dore MH (2005) Climate change and changes in global precipitation patterns: what do we know? Environ Int 31(8). ISSN 1167–1181:0160–4120. https://doi.org/10.1016/j.envint.2005.03.004
Duan Z, Bastiaanssen WGM (2017) Evaluation of three energy balance-based evaporation models for estimating monthly evaporation for five lakes using derived heat storage changes from a hysteresis model. Environ Res Lett 12(024005):1–13
Feyisa GL, Meilby H, Fensholt R, Proud SR (2014) Automated water extraction index: a new technique for surface water mapping using Landsat imagery. Remote Sens Environ 140:23–35
Genc L, Demirel K, Çamoglu G, Asik S, Smith S (2011) Determination of plant water stress using spectral reflectance measurements in watermelon (Citrullus vulgaris). Am Eurasian J Agric Environ Sci 11(2):296–304
Gorjizade A, Akhondali AM, Zarei H, Seyyed Kaboli H (2014) Evaluation of eight evaporation estimation methods in a semi-arid region (Dez reservoir, Iran). Int J Adv Biol Biomed Res 2(5):1823–1836
Ilgar R (2010) Drought status and trends in the Dardanelles and the standardized precipitation index determination. Marmara Geograph Rev 0 (22), 183
Ji L, Geng X, Sun K, Zhao Y, Gong P (2015) Target detection method for water mapping using Landsat 8 OLI/TIRS imagery. Water 7(2):794–817
Kale S, Acarlı D (2019a) Shoreline change monitoring in Atikhisar reservoir by using remote sensing and geographic information system (GIS). Fresenius Environ Bull 28(5):4329–4339
Kale S, Acarlı D (2019b) Spatial and temporal change monitoring in water surface area of Atikhisar Reservoir (Çanakkale, Turkey) by using remote sensing and geographic information system techniques. Alinteri J Agric Sci 34(1):47–56
Kapluhan E (2013) Drought and drought in turkey effect of agriculture. Int J Geogr Geogr Educat 27:487–510
Karabulut M (2015) Drought analysis in Antakya-Kahramanmaraş Graben. Turkey J Arid Land 7:741–754. https://doi.org/10.1007/s40333-015-0011-6
Karaman M, Budakoglu M, Uca Avci ZD, Özelkan E, Bülbül A, Civas M, Tasdelen S (2015) Determination of seasonal changes in wetlands using CHRIS/Proba hyperspectral satellite images: a case study from Acigöl (Denizli), Turkey. J Environ Biol 36:73–83
Karaman M (2021) Comparison of thresholding methods for shoreline extraction from Sentinel-2 and Landsat-8 imagery: Extreme Lake Salda, track of Mars on Earth. J Environ Manage 298:113481. https://doi.org/10.1016/J.JENVMAN.2021.113481
Karaman M, Özelkan E (2022) Comparative assessment of remote sensing–based water dynamic in a dam lake using a combination of Sentinel-2 data and digital elevation model. Environ Monitor Assessment 194:92. https://doi.org/10.1007/s10661-021-09703-w
Karaman M (2022) High cadence monitoring of reservoir volume fluctuations using planetScope imagery. J Hydrol 606(2022):127456. https://doi.org/10.1016/j.jhydrol.2022.127456
Koca N (2005) Environmental and economic effects of Atikhisar Dam. Eastern Geographical Review 10(14):209–233

Lang D, Zheng J, Shi J, Liao F, Ma X, Wang W, Chen X, Zhang M (2017) A comparative study of potential evapotranspiration estimation by eight methods with FAO Penman-Monteith method in Southwestern China. Water, 9(10)734: 1–18.

Li Z, Chen Y, Fang G, Li Y (2017) Multivariate assessment and attribution of droughts in Central Asia. Sci Rep 7(1316):1–12

Liu M, Liu P, Guo Y, Wang Y, Geng X, Nie Z, Yu Y (2019) Change-point analysis of precipitation and drought extremes in China over the past 50 years. Atmosphere 11(1):11. https://doi.org/10.3390/atmos11010011

Liu C, Yang C, Yang Q, Wang J (2021) Spatiotemporal drought analysis by the standardized precipitation index (SPI) and standardized precipitation evapotranspiration index (SPEI) in Sichuan Province. China. Sci Rep 11:1280. https://doi.org/10.1038/s41598-020-80527-3

McFeeters SK (1996) The use of normalized difference water index (NDWI) in the delineation of open water features. Int J Remote Sens 17(7):1425–1432

McKee TB, Doesken NJ, Kleist J (1993). The relationship of drought frequency and duration to time scales. In: Proceedings of the 8th Conference on Applied Climatology: American Meteorological Society: 17–22 January 1993, Boston, MA, USA

Mishra AK, Singh VP (2010) A review of drought concepts. J Hydrol 391(1–2):204–216

Mohammed R, Scholz M (2017) The reconnaissance drought index: a method for detecting regional arid climatic variability and potential drought risk. J Arid Environ. https://doi.org/10.1016/j.jaridenv.2017.03.014

Osuch M, Romanowicz RJ, Lawrence D, Wong WK (2016) Trends in projections of standardized precipitation indices in a future climate in Poland. Hydrol Earth Syst Sci 20:1947–1969

Özelkan E, Chen G, Üstündağ BB (2016) Multiscale object-based drought monitoring and comparison in rainfed and irrigated agriculture from Landsat 8 OLI imagery. Int J Appl Earth Observat Geoformat 44:159–170

Özelkan E, Karaman M (2018a) The Analysis of the effect of meteorological and hydrological drought on dam lake via multitemporal satellite images: a case study in Atikhisar Dam Lake (Çanakkale). Omer Halisdemir Univ J Eng Sci 7(2):1023–1037

Özelkan E, Karaman M (2018b) Hydrometeorological evaluation of urban areas in GIS platform. Sağlık A (eds), Changing and developing Laspeki urban infrastructure, Çanakkale Onsekiz Mart University, Çanakkale, s. 97–109

Özelkan E, Sağlık A, Sümer S, Bedir M, Kelkit A (2018) Examination of the effect of urbanization on agricultural areas using remote sensing – a case study in Çanakkale. COMU J Agriculture Faculty 6(1):123–135

Özelkan E (2019a) Evaluation of temporal change of dam lake area determined by remote sensing with meteorological drought: a case study in Atikhisar Dam (Çanakkale). Turkish J Agric Nat Sci 6(4):904–916. https://doi.org/10.30910/turkjans.633634

Özelkan E (2019b) Comparison of remote sensing classification techniques for water body detection: a case study in Atikhisar Dam Lake (Çanakkale). Cumhuriyet Sci J 40(3):650–661. https://doi.org/10.17776/csj.556440

Özelkan E (2020) Water body detection analysis using NDWI indices derived from Landsat-8 OLI. Polish J Environ Stud 29(2), 1759–1769. https://doi.org/10.15244/pjoes/110447

Palmer WC (1965) Meteorological drought. Office of Climatology Research Paper 45, Weather Bureau, Washington, D.C., 58 pp

Pradhan RK, Sharma D, Panda SK, Dubey SK, Sharma A (2019) Changes of precipitation regime and its indices over Rajasthan state of India: impact of climate change scenarios experiments. Clim Dyn 52:3405–3420. https://doi.org/10.1007/s00382-018-4334-9

Schultz GA, Engman ET (2012) Remote sensing in hydrology and water management. Springer, Berlin Heidelberg, Berlin, Almanya, p 483

Sener E, Davraz A, Sener S (2010) Investigation of Aksehir and Eber Lakes (SW Turkey) coastline change with multitemporal satellite images. Water Resour Manage 24(4):727–745

Şensoy S, Demircan M, Ulupınar U, Balta I (2008). Climate of Turkey. Turkish State Meteorological Service Report. https://www.mgm.gov. tr/FILES/genel/makale/13_turkiye_iklimi.pdf. Accessed 01 May 2021

TÜİK (2020) Turkish Statistical Institute Data Base. http://tuik.gov.tr/PreTabloArama.do?metod=search&araType=vt. Accessed 07 May 2021

Türkeş M (2010) Climatology and Meteorology. First Edition, Kriter Publisher – Publication No. 63, Physical Geography Series No. 1, ISBN: 978–605–5863–39–6, 650 + XXII pp., Istanbul

Tsakiris G, Vangelis H (2005) Establishing a drought index incorporation evapotranspiration Eur. Water 9(10):3–11

Veijalainen N, Ahopelto L, Marttunen M, Jääskeläinen J, Britschgi R, Orvomaa M, Belinskij A, Keskinen M (2019) Severe drought in Finland: modeling effects on water resources and assessing climate change impacts. Sustainability 11(8) 2450: 1–26

Vicente-Serrano SM, Beguería S, López-Moreno JI (2010) A multi-scalar drought index sensitive to global warming: the standardized precipitation evapotranspiration index – SPEI. J Clim 23:1696–1718

Wilhite DA (2000) Drought: a global assessment, Vol. I, edited by Donald A. Wilhite, Chap. 1, pp 3–18 (London: Routledge, 2000). http://digitalcommons.unl.edu/droughtfacpub/69

Willeke G, Hosking JRM, Wallis JR, et al (1994) The national drought atlas. In: Institute for Water Resources Report 94-NDS-4. U.S Army Corp of Engineers, CD-ROM. Norfolk, VA

Xu H (2006) Modification of normalized difference water index (NDWI) to enhance open water features in remotely sensed imagery. Int J Remote Sens 27(14):3025–3033

Yang Y, Liu Y, Zhou M, Zhang S, Zhan W, Sun C, Duan Y (2015) Landsat 8 OLI image based terrestrial water extraction from heterogeneous backgrounds using a reflectance homogenization approach. Remote Sens Environ 171:14–32

Yaykiran S, Cuceloglu G, Ekdal A (2019) Estimation of water budget components of the Sakarya River Basin by using the WEAP-PGM Model. Water, 11(2) 271: 1–17

Yetmen H (2013) Van lake basin drought analysis. Education and the Society in the 21st Century, 2(5): 184–198

Yıldız MZ, Deniz O (2005) The impacts of the level changes in closed basin lakes on the coastal settlements: the lake Van example. Fırat Univ J Soc Sci 15(1):15–31

Yolcubal I (2019) Hydrogeology Lecture Notes, Kocaeli University, Geology Department, http://jeoloji.kocaeli.edu.tr/dosyalar/dersNotlari/hidrojeoloji_ders%20notlari_prof_dr_irfan_yolcubal.pdf. Accessed 05 May 2021

Zannouni K, El Abrach H, Dhahri H, Mhimid A (2017) Study of heat and mass transfer of water evaporation in a gypsum board subjected to natural convection. Heat Mass Transfer 53(6):1911–1921

Zhou Y, Dong J, Xiao X, Xiao T, Yang Z, Zhao G, Zou Z, Qin Y (2017) Open surface water mapping algorithms: a comparison of water-related spectral indices and sensors. Water 9(4): 256, 1–16